Journal of Solid State Chemistry **163,** 275–280 (2002)
doi:10.1006/jssc.2001.9407, available online at http://www.idealibrary.com on IDEAL®

The Crystal Structure of Triuranyl Diphosphate Tetrahydrate

Andrew J. Locock[1] and Peter C. Burns

Department of Civil Engineering and Geological Sciences, University of Notre Dame, 156 Fitzpatrick Hall, Notre Dame, Indiana 46556-0767

Received July 17, 2001; in revised form September 14, 2001; accepted September 21, 2001

The hydrated neutral uranyl phosphate, $(UO_2)_3(PO_4)_2(H_2O)_4$, was synthesized by hydrothermal methods. Intensity data were collected using Mo$K\alpha$ radiation and a CCD-based area detector. The crystal structure was solved by direct methods and refined by full-matrix least-squares techniques to agreement indices $wR_2 = 0.116$ for all data, and $R1 = 0.040$, calculated for the 2764 unique observed reflections ($|F_o| \geq 4\sigma_F$). The compound is orthorhombic, space group *Pnma*, $Z = 4$, $a = 7.063(1)$ Å, $b = 17.022(3)$ Å, $c = 13.172(3)$ Å, $V = 1583.5(5)$ Å^3. The structure consists of sheets of phosphate tetrahedra and uranyl pentagonal bipyramids, with composition $[(UO_2)(PO_4)]^-$ and the uranophane sheet anion topology. The sheets are connected by a uranyl pentagonal bipyramid in the interlayer that shares corners with a phosphate tetrahedron on each of two adjacent sheets, resulting in an open framework with isolated H_2O groups in the larger cavities of the structure.

Key Words: **uranyl phosphate tetrahydrate; crystal structure refinement; powder X-ray diffraction.**

INTRODUCTION

Uranyl minerals and compounds have received considerable attention recently owing to their importance to the environment (1). They are common in the oxidized portions of U deposits and the mine and mill wastes generated as by-products of utilization of U resources (2). They form in soils contaminated by actinides (3), and are expected to be abundant alteration products of nuclear wastes in a geological repository (4–7). Actinide compounds also possess a range of physicochemical properties that provide for technological uses, and numerous recent studies have focused on the synthesis of inorganic and mixed organic–inorganic uranyl compounds (8–10, and references therein).

More than 40 uranyl phosphates have been described as minerals (2). Most species have structures that contain autunite-type sheets of vertex-sharing phosphate tetrahedra and uranyl square bipyramids, or phosphuranylite-type sheets of polymerized phosphate tetrahedra and uranyl pentagonal and hexagonal bipyramids (11, 12), although some involve chains of uranyl and phosphate tetrahedra (13). Uranyl phosphate minerals impact the mobility of U in phosphate-rich rocks and aquifers, such as in the Koongarra U deposit in Australia (14), and the soils of the Fernald site in Ohio (3). Despite the significance of these minerals, fewer than half of the known species have had their structures refined.

The compound $(UO_2)_3(PO_4)_2(H_2O)_4$ has been known for at least half a century (15). It is the stable crystalline phase in the system UO_3–H_2O–H_3PO_4 at standard temperature and pressure and low phosphate concentrations, < 0.014 M $\sum PO_4^{3-}$ (16, 17). It is easily produced by boiling $(H_3O)[(UO_2)(PO_4)](H_2O)_3$ (the mineral chernikovite) in water followed by drying in air (18–20), or by washing with toluene or acetone (20). The ease of synthesis by alteration of chernikovite leads us to suspect that $(UO_2)_3(PO_4)_2(H_2O)_4$ may be an important phase in some natural systems, although it has not been reported as a mineral, and that it may form due to alteration of nuclear waste in the presence of phosphate.

Numerous studies of $(UO_2)_3(PO_4)_2(H_2O)_4$ have investigated its chemical composition (16, 17, 19–21), powder X-ray diffraction characteristics (17, 20–22), differential thermal and thermogravimetric behavior (17, 20, 21, 23), infrared spectra (17, 20, 21), Raman spectra (20), and crystal morphology (20). Satisfactory crystals for a single-crystal study have apparently not been previously obtained, and the structure has never been reported. We have developed a new synthesis method that yields excellent single crystals of $(UO_2)_3(PO_4)_2(H_2O)_4$ and we report its crystal structure herein.

EXPERIMENT

Crystal Synthesis

Single crystals of $(UO_2)_3(PO_4)_2(H_2O)_4$ were obtained by hydrothermal reaction of 0.079 g of natural fluorapatite, ideally $Ca_5(PO_4)_3F$, from the Liscombe Deposit, near Wilberforce, Ontario, Canada, with 0.15 g of concentrated HNO_3 (Fisher), 0.047 g of $UO_2(NO_3)_2(H_2O)_6$ (Alfa), and

[1] To whom correspondence should be addressed. Facsimile: 219 247 1206. E-mail: alocock@nd.edu.

0022-4596/02 $35.00

4.75 g of ultrapure H_2O. The reactants were weighed into a Teflon-lined Parr bomb and heated at 140(1)°C in a Fisher Isotemp oven for 13 days. The Parr bomb was then removed to air and allowed to cool to room temperature. The products were filtered and washed with ultrapure water, and consisted of a feltlike mass of pale yellow translucent needles of $(UO_2)_3(PO_4)_2(H_2O)_4$. The needles range up to 0.5 mm in length, and fluoresce a weak greenish-yellow color under short-wave ultraviolet (254 nm) illumination, but remain dark under long-wave ultraviolet light (365 nm). The yield of the reaction was calculated on the basis of uranium content to be 70%.

Powder X-Ray Diffraction

An aliquot of the $(UO_2)_3(PO_4)_2(H_2O)_4$ needles was ground under acetone and mounted onto an off-cut single-crystal Si wafer. A powder X-ray diffraction pattern was collected from 5 to 60°2θ using a Rigaku Miniflex diffractometer at room temperature and the following conditions: Cu$K\alpha$ radiation, Ni filter, NaI(Tl) detector, $\theta/2\theta$ geometry, continuous scan at 2° 2θ/minute, sampling width 0.01° 2θ, 30 keV, 15 mA, variable divergence slit, and 0.3 mm receiving slit. The pattern obtained was examined using JADE 3.1 software and compared to the ICDD's Powder Diffraction File Database Sets 1–47.

Optical Properties

A Zeiss binocular petrographic microscope, white light, and Cargille refractive index fluids were used to determine the refractive indices of $(UO_2)_3(PO_4)_2(H_2O)_4$ by the immersion method. The principal refractive indices determined—$n_\alpha = 1.600(4)$ and $n_\gamma = 1.638(4)$—are in contrast to those previously reported for this compound (21): $n_\alpha = 1.57$ and $n_\gamma = 1.581$. However, these latter refractive indices perfectly match those of chernikovite, $(H_3O)[(UO_2)(PO_4)](H_2O)_3$ (24), which was reported to occur together with $(UO_2)_3(PO_4)_2(H_2O)_4$ in the same synthesis (21).

Single-Crystal X-Ray Diffraction

A suitable crystal of $(UO_2)_3(PO_4)_2(H_2O)_4$ was mounted on a Bruker PLATFORM three-circle X-ray diffractometer operated at 50 keV and 40 mA and equipped with a 4 K APEX CCD detector with a crystal to detector distance of 4.7 cm. A sphere of three-dimensional data was collected using graphite-monochromatized Mo$K\alpha$ X-radiation and frame widths of 0.3° in ω, with 40 seconds count-time per frame. Data were collected for $4^\circ < 2\theta < 69^\circ$ in ~30.5 hours; comparison of the intensities of equivalent reflections measured at different times during data collection showed no significant decay. The unit cell (Table 1) was refined with 7981 reflections using least-squares techniques. The intensity data were reduced and corrected for Lorentz, polarization, and background effects using the Bruker program SAINT. A semiempirical absorption correction was applied by modeling the crystal as an ellipsoid, and lowered R_{INT} of 4741 intense reflections from 0.096 to 0.042. Systematic absences of reflections were consistent with space groups $Pna2_1$ and *Pnma*, and assigning phases to a set of normalized structure factors gave a mean value of $|E^2 - 1|$ of 1.004, consistent with space group *Pnma*. A total of 32,351 intensities was collected, of which 1813 were discarded as being inconsistent with the space group; 13 of these intensities were classified as observed, corresponding to 4 unique reflections. Of the 30,538 remaining intensities, 3413 were unique ($R_{INT} = 0.056$), of which 2764 were classified as observed reflections ($|F_o| \geq 4\sigma_F$). Scattering curves for neutral atoms, together with anomalous dispersion corrections, were taken from *International Tables for X-ray Crystallography*, Volume IV (25). The Bruker SHELXTL Version 5 (26) series of programs was used for the solution and refinement of the crystal structure.

TABLE 1
Crystallographic Data and Details of the Structure Refinement for $(UO_2)_3(PO_4)_2(H_2O)_4$

a (Å)	7.063(1)
b (Å)	17.022(3)
c (Å)	13.172(3)
V (Å^3)	1583.5(5)
Space group	*Pnma*
Temperature (K)	293(2)
Formula	$(UO_2)_3(PO_4)_2(H_2O)_4$
Formula weight (g/mol)	1072.09(8)
Z	4
Wavelength (Å)	0.71073
$F(000)$	1832
μ (mm^{-1})	30.90
D_{calc} (g/cm^3)	4.497(2)
Crystal size (mm)	$0.02 \times 0.02 \times 0.33$
θ range of data collection	1.95 to 34.50°
Data collected	$-11 \leq h \leq 11$, $-27 \leq k \leq 26$, $-20 \leq l \leq 20$
Total reflections	30,538
Unique reflections	3413
R_{int}	0.056
Unique $\lvert F_o\rvert \geq 4\sigma_F$	2764
Completeness to $\theta = 34.5°$	99.0%
Refinement method	Full-matrix least-squares on F^2
Parameters varied	112
$R1$,[a] for $\lvert F_o\rvert \geq 4\sigma_F$	0.040
$R1$,[a] all data	0.048
wR_2,[b] all data	0.116
Goodness of fit, all data	1.322
Max., min. peaks (e/Å^3)	3.94, −2.55

[a] $R1 = [\sum\|F_o| - |F_c\|]/\sum|F_o|$. [b] $wR_2 = [\sum[w(F_o^2 - F_c^2)^2]/\sum[w(F_o^2)^2]]^{0.5}$.

TABLE 2
Atomic Coordinates ($\times 10^4$) and Displacement Parameters ($Å^2 \times 10^3$) for $(UO_2)_3(PO_4)_2(H_2O)_4$

	x	y	z	U_{eq}	U_{11}	U_{22}	U_{33}	U_{23}	U_{13}	U_{12}
U(1)	7408(1)	5210(1)	1773(1)	12(1)	9(1)	18(1)	10(1)	0(1)	0(1)	0(1)
U(2)	6564(1)	7500	4789(1)	21(1)	28(1)	14(1)	20(1)	0	0(1)	0
P(1)	7421(3)	5397(1)	4158(2)	10(1)	10(1)	13(1)	8(1)	0(1)	0(1)	1(1)
O(1)	7363(11)	6243(5)	1725(6)	21(2)	22(4)	21(4)	21(4)	0(3)	1(3)	−2(3)
O(2)	7419(10)	4799(4)	5032(5)	15(1)	15(3)	19(3)	10(3)	3(3)	−1(2)	0(3)
O(3)	5726(10)	5247(5)	3429(5)	17(1)	8(3)	34(4)	11(3)	0(3)	−1(2)	3(3)
O(4)	9103(10)	5246(5)	3433(5)	17(1)	7(3)	34(4)	11(3)	0(3)	2(2)	−3(3)
O(5)	7403(14)	4158(5)	1840(8)	31(2)	40(5)	19(4)	34(5)	2(4)	−2(4)	−1(4)
O(6)	7443(13)	6223(5)	4541(7)	25(2)	36(5)	13(3)	26(4)	−6(3)	1(4)	1(3)
O(7)	7710(20)	7500	6005(11)	33(3)	39(8)	21(6)	39(8)	0	−11(6)	0
O(8)	5370(20)	7500	3639(11)	36(3)	40(8)	31(7)	36(8)	0	−11(6)	0
O(9)	4022(16)	6695(6)	5585(9)	43(3)	45(6)	24(5)	59(7)	−3(5)	11(5)	−9(4)
O(10)	9700(20)	7500	3929(15)	51(5)	50(9)	13(6)	91(14)	0	33(10)	0
O(11)	1530(30)	7500	6847(16)	97(10)	51(13)	200(30)	42(11)	0	7(10)	0

Note. U_{eq} is defined as one-third of the trace of the orthogonalized U_{ij} tensor. The anisotropic displacement parameter exponent takes the form $-2\pi^2[h^2a^{*2}U_{11} + \cdots + 2hka^*b^*U_{12}]$.

STRUCTURE SOLUTION AND REFINEMENT

The structure was solved by direct methods and was refined successfully based on F^2 for all unique data in space group *Pnma*. A structure model including anisotropic displacement parameters for all atoms converged, and gave an agreement index ($R1$) of 0.040, calculated for the 2764 observed unique reflections ($|F_o| \geq 4\sigma_F$). The final value of wR_2 was 0.116 for all data using the structure factor weights assigned during least-squares refinement: $a = 0.0245$ and $b = 56.66$, where $wR_2 = [\sum[w(F_o^2 - F_c^2)^2]/\sum[w(F_o^2)^2]]^{0.5}$, $w = 1/(\sigma^2(F_o^2) + (aP)^2 + bP)$, and $P = \frac{1}{3}\max(0, F_o^2) + \frac{2}{3}F_c^2$. In the final cycle of refinement the mean parameter shift/esd was 0.000, and the maximum peaks in the final difference Fourier maps were 3.94 and $-2.55\,e/Å^3$. The atomic positional parameters and displacement parameters are given in Table 2, and selected interatomic distances and angles are given in Table 3. The locations of the H atoms in the unit cell were not determined. Observed and calculated structure factors are available from the National Auxiliary Publications Service.[2]

TABLE 3
Selected Interatomic Distances (Å) and Angles (°) for $(UO_2)_3(PO_4)_2(H_2O)_4$

U(1)–O(1)	1.759(8)		
U(1)–O(5)	1.793(9)	O(1)–U(1)–O(5)	178.6(4)
U(1)–O(2)a	2.297(7)	O(1)–U(1)–O(2)a	88.4(3)
U(1)–O(4)b	2.351(7)	O(1)–U(1)–O(4)b	87.3(3)
U(1)–O(3)c	2.359(7)	O(1)–U(1)–O(3)c	89.3(3)
U(1)–O(3)	2.484(7)	O(1)–U(1)–O(3)	89.9(3)
U(1)–O(4)	2.493(7)	O(1)–U(1)–O(4)	90.9(3)
⟨U(1)–O⟩	2.219		
U(2)–O(8)	1.734(14)		
U(2)–O(7)	1.794(14)	O(8)–U(2)–O(7)	177.7(7)
U(2)–O(6)d	2.284(8)	O(8)–U(2)–O(6)d	90.4(3)
U(2)–O(6)	2.284(8)	O(8)–U(2)–O(6)	90.4(3)
U(2)–O(10)	2.489(16)	O(8)–U(2)–O(10)	92.0(8)
U(2)–O(9)d	2.490(10)	O(8)–U(2)–O(9)d	91.0(5)
U(2)–O(9)	2.490(11)	O(8)–U(2)–O(9)	91.0(5)
⟨U(2)–O⟩	2.224		
P–O(6)	1.495(8)	O(6)–P(1)–O(2)	111.7(5)
P–O(2)	1.537(7)	O(6)–P(1)–O(4)	110.9(5)
P–O(4)	1.546(7)	O(6)–P(1)–O(3)	111.8(5)
P–O(3)	1.556(7)	O(2)–P(1)–O(3)	110.7(4)
⟨P–O⟩	1.533	O(2)–P(1)–O(4)	110.7(4)
		O(4)–P(1)–O(3)	100.5(4)

Note. Symmetry transformations used to generate equivalent atoms: a $= -x + \frac{3}{2}, -y + 1, z - \frac{1}{2}$; b $= x - \frac{1}{2}, y, -z + \frac{1}{2}$; c $= x + \frac{1}{2}, y, -z + \frac{1}{2}$; d $= x, -y + \frac{3}{2}, z$.

The powder X-ray diffraction pattern of $(UO_2)_3(PO_4)_2(H_2O)_4$ was calculated using the program ATOMS version 5.1 (27) and the structural parameters from the single-crystal structure refinement. The simulated pattern yielded *d*-spacings whose positions are in agreement with the measured pattern (Table 4) and with the ICDD's Powder Diffraction File cards 37-0369, 30-1405, and 13-0039. The relative intensities of the measured *d*-spacings are in good agreement with previously published patterns (17, 20–22), but differ

[2] See NAPS document No. 05606 for 10 pages of supplementary material. This is not a multiarticle document. Order from NAPS c/o Microfiche Publications, 248 Hempstead Turnpike, West Hempstead, NY 11552. Remit in advance in U.S. funds only $7.75 for photocopies or $5.00 for microfiche. There is a $25.00 invoicing charge on all orders filled before payment. Outside U.S. and Canada please add $4.50 for the first 20 pages and $1.00 for each 10 pages of material thereafter, or $5.00 for the first microfiche and $1.00 for each microfiche thereafter.

TABLE 4
Calculated and Measured *d*-Spacings and Relative Intensities for the 25 Most Intense Lines Calculated

h	*k*	*l*	d_{calc}	I_{calc}	d_{meas}	I_{meas}
0	1	1	10.417	22	10.285	5
0	2	0	8.511	64	8.412	37
1	0	1	6.224	13		
1	1	1	5.846	43	5.781	1
0	3	1	5.211	14		
0	2	2	5.209	100	5.169	78
1	2	1	5.024	16		
1	0	2	4.817	22		
0	4	0	4.255	71	4.228	100
1	3	1	4.193	25		
1	2	2	4.192	61		
1	1	3	3.643	22	3.615	1
2	0	0	3.531	42		
0	5	1	3.296	15	3.279	18
2	2	0	3.262	28		
0	2	4	3.071	11	3.054	9
1	0	4	2.985	49	2.967	4
2	2	2	2.923	17		
1	2	4	2.816	29	2.799	3
2	4	0	2.718	16		
1	5	3	2.514	18	2.502	3
1	4	4	2.444	19	2.433	7
1	7	1	2.265	13	2.256	6
3	2	4	1.868	18	1.862	22
1	9	3	1.687	13	1.683	8

Note. Blank spaces indicate that the intensity of the line was below detection.

substantially from the simulated pattern; this is interpreted to be a result of severe preferred orientation of the $(UO_2)_3(PO_4)_2(H_2O)_4$ needles in the powder examined.

RESULTS

Structure Description

There are two symmetrically independent U atoms in $(UO_2)_3(PO_4)_2(H_2O)_4$, each of which are part of an approximately linear $(UO_2)^{2+}$ cation. Both uranyl ions are coordinated by five additional anions arranged at the equatorial positions of pentagonal bipyramids, with the uranyl O atoms at the apices of the bipyramids. The equatorial anions of U(1) consist of five O atoms, whereas the equatorial anions of U(2) consist of two O atoms and three H_2O groups.

The U(1) pentagonal bipyramids share equatorial edges, giving a chain of bipyramids that is one polyhedron wide. Topologically identical chains of uranyl polyhedra are common in uranyl compounds (11). Phosphate tetrahedra are attached to either side of the chains by sharing edges with the uranyl polyhedra (Fig. 1); within any uranyl phosphate chain, the orientations of all phosphate tetrahedra are identical. Translationally equivalent uranyl phosphate chains are joined by the sharing of equatorial vertices of uranyl pentagonal bipyramids with phosphate tetrahedra from adjacent chains, resulting in sheets that are parallel to (010). The anion topology of the uranyl phosphate sheet, derived by the method of Burns *et al.* (11), is the same as that of uranophane, $Ca[(UO_2)SiO_3(OH)]_2(H_2O)_5$, and is shown in Fig. 2. Many structures of uranyl compounds contain sheets based upon this anion topology (11), with the pentagons populated by uranyl ions, and the triangles by tetrahedra or triangles, or the squares by distorted tetrahedra or octahedra. However, the cant of the phosphate tetrahedra in $(UO_2)_3(PO_4)_2(H_2O)_4$ is novel; for a given uranyl polyhedral chain within the sheet, all of the tetrahedra point in the same direction, in contrast to the alternating geometry of the tetrahedra observed in other compounds with the uranophane sheet anion topology (11).

The U(2) pentagonal bipyramid is located in the interlayer, between the uranyl phosphate sheets. Two equatorial oxygens of the U(2) pentagonal bipyramid are shared with phosphate tetrahedra, linking the uranyl phosphate sheets, and resulting in an open-framework structure (Fig. 3). The coordination polyhedron about U(2) is completed by three

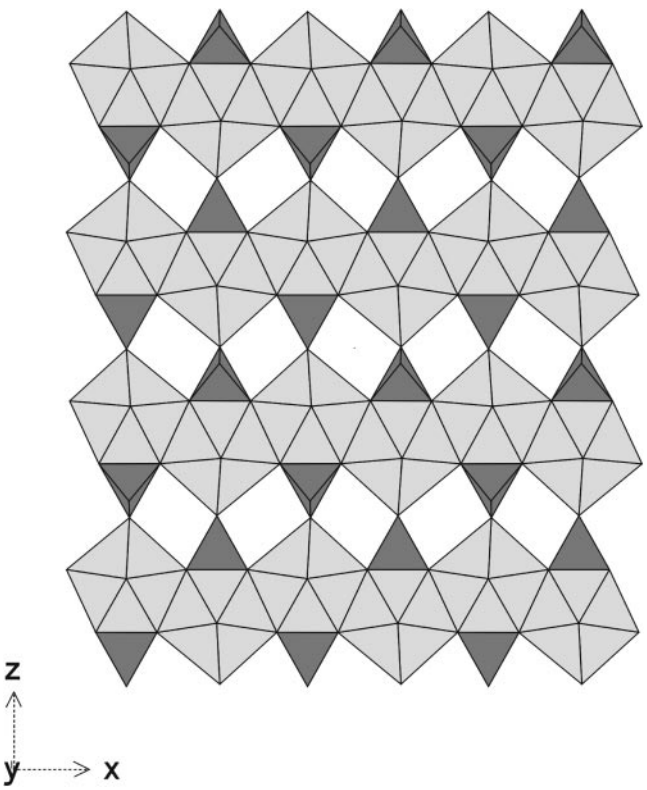

FIG. 1. Polyhedral representation of the uranyl phosphate sheet of $(UO_2)_3(PO_4)_2(H_2O)_4$ projected along [010]. The sheets have the composition $[(UO_2)(PO_4)]^-$. The uranyl polyhedra are shown in light gray and the phosphate tetrahedra are shown in dark gray.

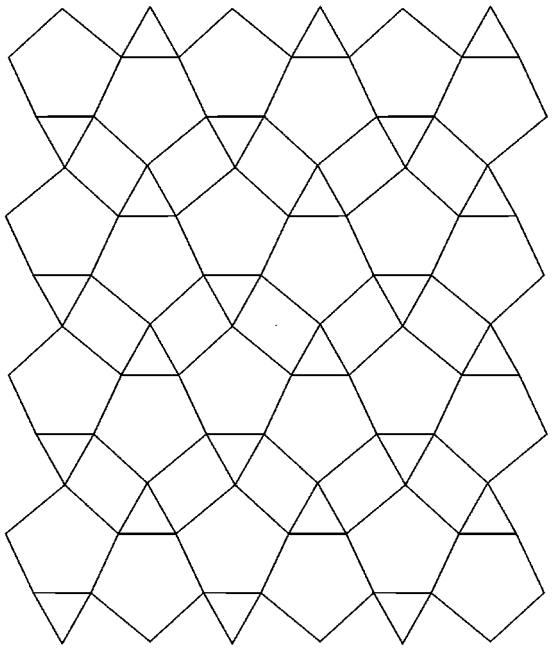

FIG. 2. Sheet anion topology of $(UO_2)_3(PO_4)_2(H_2O)_4$; it is identical to that of uranophane, $Ca[(UO_2)SiO_3(OH)]_2(H_2O)_5$.

H_2O groups, and additional H_2O groups occupy the larger cavities of the structure.

Bond Valence Analysis

The bond valence sums at the cation sites, calculated using the parameters of Burns *et al.* (28) for $^{[7]}U^{6+}$, and Brown and Altermatt (29) for P, are 5.93, 5.98, and 5.03 valence units for U(1), U(2), and P, respectively. These results are consistent with formal valences of U^{6+} and P^{5+}. The bond valence sums for the H_2O groups are 0.42, 0.42, and 0.00 valence unit for O(9), O(10), and O(11), respectively, in accord with their assignment as water. The bond valence sums of the remaining O atoms ranged from 1.63 to 2.02 valence units.

DISCUSSION

The structure of $(UO_2)_3(PO_4)_2(H_2O)_4$ possesses a novel uranyl phosphate open-framework structure. It is the first inorganic structure with uranyl phosphate sheets based on the uranophane sheet anion topology. Several nonphosphate uranyl compounds contain sheets based upon an identical anion topology (11, 12). These sheets invariably involve population of the pentagons of the underlying anion topology with uranyl ions, resulting in uranyl pentagonal bipyramids. In the majority of the structures, the triangular sites of the anion topology are populated by triangles or tetrahedra, as is the case in $(UO_2)_3(PO_4)_2(H_2O)_4$, with the tetrahedra oriented such that one face of the tetrahedron corresponds to the triangle in the anion topology, and one tetrahedral ligand is only singly connected within the sheet. In a few structures, the triangle in the anion topology is vacant; in these cases, the square site is occupied by a distorted tetrahedron, or corresponds to the equatorial vertices of an octahedron (12, 30).

The uranyl phosphate sheets found in the mixed organic–inorganic compounds $[NHEt_3][(UO_2)_2(PO_4)(HPO_4)]$ and $[NPr_4][(UO_2)_3(PO_4)(HPO_4)_2]$ (8) are also based upon the uranophane sheet anion topology. The sheets differ from those found in $(UO_2)_3(PO_4)_2(H_2O)_4$ in the orientation of the phosphate tetrahedra, which alternate up and down along either side of the uranyl polyhedral chain in these organic–inorganic compounds.

Uranyl phosphate frameworks, such as that found in $(UO_2)_3(PO_4)_2(H_2O)_4$, are uncommon; we are not aware of others having been produced synthetically. However, there

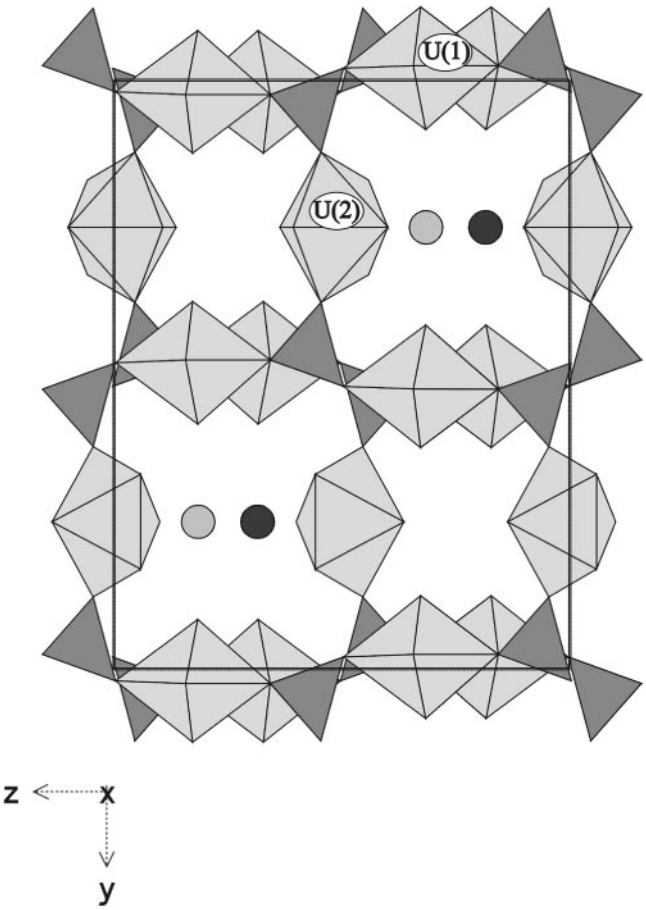

FIG. 3. Polyhedral representation of the structure of $(UO_2)_3(PO_4)_2(H_2O)_4$ projected along [100]. The uranyl polyhedra are shown in light gray and the phosphate tetrahedra are shown in dark gray. The isolated water molecules in the structure are shown as spheres shaded pale gray to indicate displacement toward the observer, and dark gray to indicate displacement away from the observer.

are natural examples, including the minerals phosphuranylite $[KCa(H_3O)_3(UO_2)[(UO_2)_3(PO_4)_2O_2]_2(H_2O)_8]$, althupite $[AlTh(UO_2)[(UO_2)_3(PO_4)_2O(OH)]_2(OH)_3(H_2O)_{15}]$, vanmeersscheite $[U(OH)_4[(UO_2)_3(PO_4)_2(OH)_2]_2(H_2O)_4]$, and metavanmeersscheite $[U(OH)_4[(UO_2)_3(PO_4)_2(OH)_2]_2(H_2O)_2]$, which contain sheets of uranyl pentagonal and hexagonal bipyramids that are linked into a framework by sharing vertices with uranyl polyhedra located in the interlayer of the structure. The various structural sites in cavities within the frameworks of these minerals are occupied by low-valence cations and H_2O groups.

ACKNOWLEDGMENTS

This research was funded by the Environmental Management Sciences Program of the United States Department of Energy (DE-FGO7-97ER14820). Yaping Li is thanked for his assistance with the hydrothermal synthesis.

REFERENCES

1. P. C. Burns and R. J. Finch, Eds., *Rev. Mineral.* **38** (1999).
2. R. J. Finch and T. Murukami, *Rev. Mineral.* **38,** 91–179 (1999).
3. E. C. Buck, N. R. Brown, and N. L. Dietz, *Environ. Sci. Technol.* **30,** 81–88 (1996).
4. E. C. Buck, D. J. Wronkiewicz, P. A. Finn, and J. K. Bates, *J. Nucl. Mater.* **249,** 70–76 (1997).
5. P. A. Finn, J. C. Hoh, S. F. Wolf, S. A. Slater, and J. K. Bates, *Radiochim. Acta* **74,** 65–71 (1996).
6. R. J. Finch, E. C. Buck, P. A. Finn, and J. K. Bates, *Mater. Res. Soc. Symp. Proc.* **556,** 431–438 (1999).
7. P. C. Burns, R. A. Olson, R. J. Finch, J. M. Hanchar, and Y. Thibault, *J. Nucl. Mater.* **278,** 290–300 (2000).
8. R. J. Francis, M. J. Drewitt, P. S. Halasyamani, C. Ranganathachar, D. O'Hare, W. Clegg, and S. J. Teat, *Chem. Commun.* 279–280 (1998).
9. A. C. Bean, S. M. Peper, and T. E. Albrect-Schmitt, *Chem. Mater.* **13,** 1266–1272 (2001).
10. C. L. Cahill and P. C. Burns, *Inorg. Chem.* **40,** 1347–1351 (2001).
11. P. C. Burns, M. L. Miller, and R. C. Ewing, *Can. Mineral.* **34,** 845–880 (1996).
12. P. C. Burns, *Rev. Mineral.* **38,** 23–90 (1999).
13. P. C. Burns, *Am. Mineral.* **85,** 801–805 (2000).
14. T. Murakami, T. Ohnuki, H. Isobe, and T. Sato, *Am. Mineral.* **82,** 88–899 (1997).
15. A. D. Ryon and D. W. Kuhn, Report Y-315, January 10, 1949, cited in (16).
16. J. M. Schreyer and C. F. Baes, Jr., *J. Am. Chem. Soc.* **76,** 354–357 (1954).
17. L. V. Kobets, T. A. Kolevich, and D. S. Umreiko, *Russ. J. Inorg. Chem.* (*Transl. of Zh. Neorg. Khim.*) **23,** 501–505 (1978).
18. L. V. Kobets and D. S. Umreiko, *Russ. Chem. Rev.* (*Engl. Transl.*) **52,** 509–523 (1983).
19. F. Weigel and G. Hoffmann, *J. Less-Common Met.* **44,** 99–123 (1976).
20. M. Pham-Thi and Ph. Colomban, *J. Less-Common Met.* **108,** 189–216 (1985).
21. G. A. Sidorenko, I. G. Zhil'tsova, I. Kh. Moroz, and A. A. Valuyeva, *Dokl. Akad. Nauk SSSR* (*Engl. Transl.*) **222,** 124–127 (1975).
22. H. W. Dunn, ORNL-2092, 10 (1956), cited in (17).
23. J. M. Schaekers, *J. Therm. Anal.* **6,** 543–554 (1974).
24. J. W. Anthony, R. A. Bideaux, K. W. Bladh, and M. C. Nichols, "Handbook of Mineralogy," Vol. IV, p. 107, Mineral Data Publishing, Tucson, AZ, 2000.
25. J. A. Ibers and W. C. Hamilton, Eds., "International Tables for X-ray Crystallography," Vol. IV, Kynoch Press, Birmingham, UK, 1974.
26. "SHELXTL NT, Program Suite for Solution and Refinement of Crystal Structures," version 5.1. Bruker Analytical X-ray Systems, Madison, WI, 1998.
27. E. Dowty, "ATOMS for Windows and Macintosh," version 5.1. Shape Software, Kingsport, TN, 2000.
28. P. C. Burns, R. C. Ewing, and F. C. Hawthorne, *Can. Mineral.* **35,** 1551–1570 (1997).
29. I. D. Brown and D. Altermatt, *Acta Crystallogr. B* **41,** 244–247 (1985).
30. S. V. Krivovichev and P. C. Burns, *Can. Mineral.* **38,** 717–726 (2000).